Journal of Orthopaedic Translation 22 (2020) 109–115

Contents lists available at ScienceDirect

Journal of Orthopaedic Translation

journal homepage: www.journals.elsevier.com/journal-of-orthopaedic-translation

Original Article

Three-dimensional distribution of cystic lesions in osteonecrosis of the femoral head

Guang-Bo Liu [a,☆], Rui Li [a,☆], Qiang Lu [a], Hai-Yang Ma [a], Yu-Xuan Zhang [a], Qi Quan [a], Xue-Zhen Liang [b], Jiang Peng [a,**], Shi-Bi Lu [a,*]

[a] Institute of Orthopedics, Beijing Key Laboratory of Regenerative Medicine in Orthopedics, Key Laboratory of Musculoskeletal Trauma & War Injuries PLA, Chinese PLA General Hospital, Beijing, 100853, China

[b] The First Clinical Medical School, Shandong University of Traditional Chinese Medicine, Shandong, 250355, China

ARTICLE INFO

Keywords:
Computed tomography
Cystic lesions
Osteonecrosis of the femoral head
Three-dimensional distribution

ABSTRACT

Purpose: The aim of this study was to investigate the location characteristics of cystic lesions in a three-dimensional context and discuss the mechanism of formation.

Methods: A total of 155 femoral head computed tomography images from 94 patients diagnosed with stage II and III osteonecrosis of the femoral head were retrospectively reviewed. Three-dimensional structures of the femoral head including the cystic lesions and necrotic area were reconstructed. We divided each femoral head into eight regions to observe the positional relationship of the cystic lesions, normal areas, and necrotic areas.

Results: The regional distribution revealed 14 (13%), 35 (32%), 9 (8%), 25 (23%), 6 (6%), 15 (14%), 4 (4%), and 0 (0%) cystic lesions in regions I, II, III, IV, V, VI, VII, and VIII, respectively. The anteromedial zone, A (I + III), contained 22% of the lesions, anterolateral zone, B (II + IV), contained 54%, posteromedial zone, C (V +VII), contained 9% of the lesions, and posterolateral zone, D (VI + VIII), contained 15% of the lesions. Most of the cystic lesions (78%) were located between the normal and necrotic areas; 18% of cystic lesions were in the necrotic area and 4% were in the normal area.

Conclusions: Cystic lesions most often occur at the junction of the necrotic and normal areas and are most commonly located in the anterolateral femoral head, which is similar to the distribution of the stress concentration region.

The translational potential of this article: The study showed the location characteristics of cystic lesions in osteonecrosis of femoral head, which suggested that the formation of cystic lesions may be related to stress and could accelerate the collapse of femoral head. The results can support further research on cystic lesions and provide a reference for doctors' treatment strategies for patients with osteonecrosis of femoral head.

Introduction

Osteonecrosis of the femoral head (ONFH) is considered a challenging disease that is induced by insufficient blood supply, although the pathological mechanism of ischaemia is still unknown [1–3]. Collapse of the femoral head is considered to be an important event because it can lead to secondary osteoarthritis (OA) with severe pain and dysfunction [4,5]. There are many factors that can affect collapse, such as the extent of the osteonecrotic lesion and the location of the lesion [3]. Studies on patients with ONFH have found that cystic lesions are also closely related to collapse, but at present, the research on cystic lesions in ONFH remains limited [6,7].

Cystic lesions are considered a typical sign of stage II ONFH according to the Association Research Circulation Osseous staging system, as determined by the radiological appearance of a translucent area [8]. The pathologic characteristics of cystic lesions, including the presence of single or multiple lesions within the necrotic area, are noncavitary and contain loose fibrous elements [9,10]. However, in terms of the location characteristics of cystic lesions, the findings are

* Corresponding author.
** Corresponding author.
E-mail addresses: dr_liuguangbo@126.com (G.-B. Liu), ryanlee301@163.com (R. Li), 13911595980@163.com (Q. Lu), Mahaiyang822@163.com (H.-Y. Ma), 51013685@qq.com (Y.-X. Zhang), zenkii@126.com (Q. Quan), liangxz0429@163.com (X.-Z. Liang), pengjdxx@126.com (J. Peng), lushibi301@126.com (S.-B. Lu).
☆ **Co-first author:** The first two authors contributed equally to this work and are considered co-first author.

https://doi.org/10.1016/j.jot.2019.10.010
Received 11 July 2019; Received in revised form 16 October 2019; Accepted 21 October 2019
Available online 14 November 2019

quite limited. A study based on X-ray images showed that cystic lesions were identified within the necrotic area, particularly along the lateral margin of the femoral head [10]. Another study based on computed tomography (CT) images indicated that the anterior area and central pillar were the main areas of distribution of cystic lesions in the hips of patients with ONFH, and cystic lesions are often found near the sclerosis rim in ONFH [6]. However, although this study was based on CT images, the analysis was only based on specific layers and thus, based on two-dimensional images rather than three-dimensional images. From our point of view, location information from two-dimensional images will inevitably be insufficient or even inaccurate because it can only reflect the distribution at a certain level; these images cannot provide a clear full view of the distribution of the cystic lesions. To the best of our knowledge, no study has been published investigating this issue in a three-dimensional space.

Therefore, the purpose of this study was to reconstruct the cystic lesions, necrotic areas, and femoral heads in a three-dimensional space and analyse the distribution of cystic lesions in the femoral head and the relative positional relationship among cystic lesions, normal areas, and necrotic areas. In addition, with a reference to the formation mechanism of cystic lesion in OA, we discuss cystic lesion formation in ONFH and assume that the formation of cystic lesions may relate to stress.

Materials and methods

Our institution's research ethics board approved this study. Using the picture archiving and communication system of the Chinese People's Liberation Army General Hospital, we retrospectively reviewed CT data from 120 consecutive patients with ONFH scanned between April 2014 and September 2018; the scans had a slice thickness of $\leq$1 mm, a slice increment of $\leq$0.6 mm, and a pixel size of $\leq$0.8 mm. All of these patients were at stages II or III according to the Association Research Circulation Osseous classification systems. Eight patients without CT data and 18 patients who had undergone surgical treatment of the ONFH hip were excluded. Ultimately, 94 patients (155 hips) were included in this study.

Three-dimensional reconstruction of the femur, necrotic areas, and cystic lesions

Row hip CT data were obtained in the axial plane and imported to the Mimics software (version 21.0; Materialise, Leuven, Belgium). First, using a software tool based on Hounsfield units, which are related to intensity, a rough femoral head construction was acquired. Then, the structural details of the femoral head were refined by tracing the outline of the femoral head manually at each level (Figure 1A). Based on the

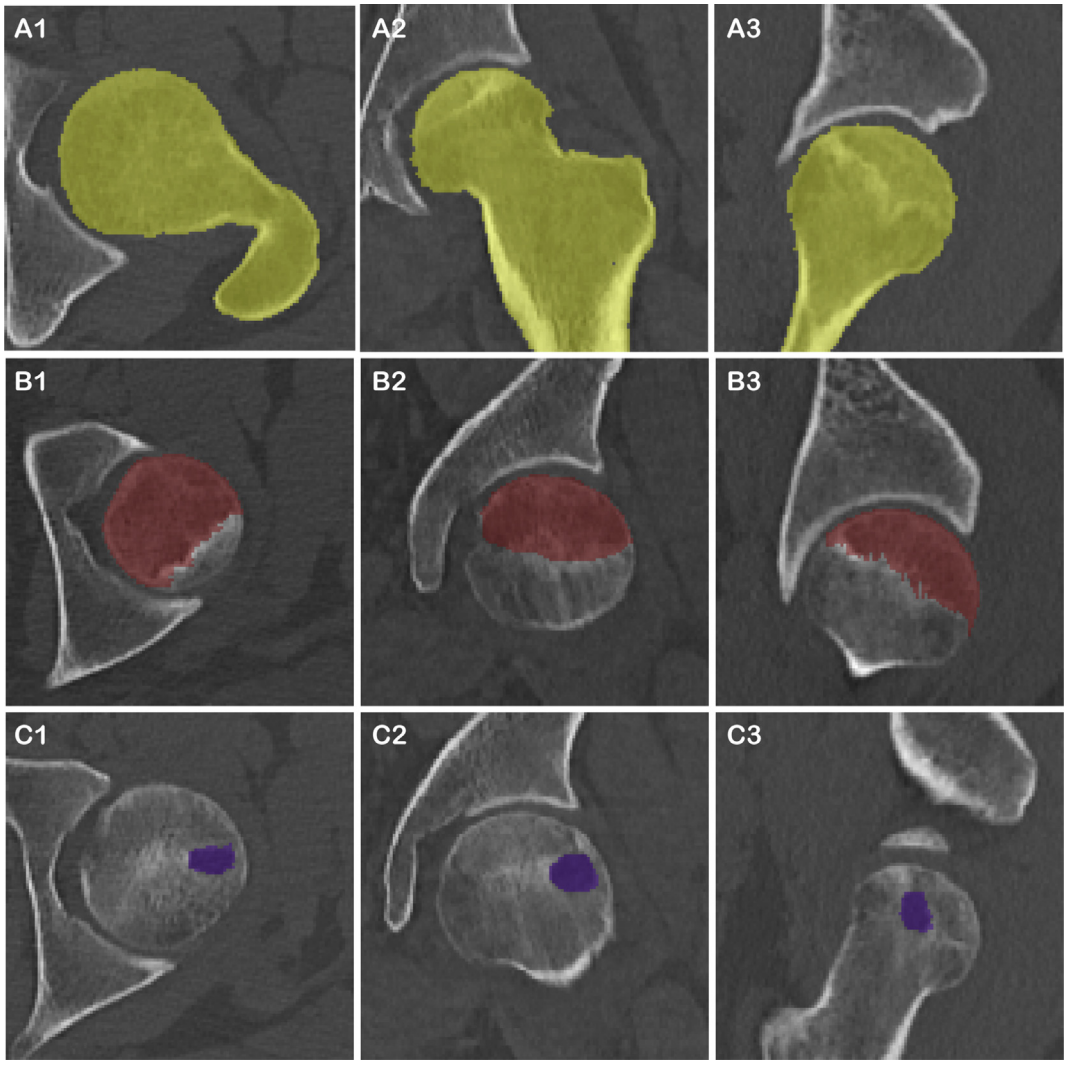

Figure 1. Selection of the regions of interest in the CT images. (A1-A3) The contour of each femoral layer is obtained by software semiautomatic tools and manual addition and subtraction. The yellow area is the femoral head area at a certain level. (B1–B3) The location and definition of the necrotic area. The red area is a necrotic area at a certain level. (C1–C3) The location and definition of cystic lesions. The purple area is a cystic lesion at a certain level. (For interpretation of the references to colour in this figure legend, the reader is referred to the Web version of this article.)

reduced bone density of the necrotic zone compared with the normal zone, we manually segmented the necrotic area at each level using the previously described method (Figure 1B) [11,12]. Cystic lesions in which the bone structure was no longer present were also segmented based on differences in density (Figure 1C). After the femoral head, cystic lesions and necrotic areas were segmented at each CT level, a corresponding three-dimensional object was then created in Mimics software. Finally, the three resulting objects (femoral head, necrotic areas, and cystic lesions) were smoothed in Mimics to obtain an optimally homogeneous and anatomically faithful three-dimensional structure (Figure 2).

Radiographic analysis

To determine the distribution of cystic lesions on the femoral head, we divided the femoral head into eight regions through three mutually perpendicular planes. The partitions were defined according to the previous reports [7,13]. Initially, Plane 1 was obtained, which included the centre of the femoral head, the centre of the femoral head fovea, and the centre of the calcar. Plane 2 was perpendicular to Plane 1 and passed through the centre of the femoral head and the centre of femoral head fovea. Plane 3 passed through the centre of the femoral head and was perpendicular to Plane 1 and Plane 2 (Figure 3). The femoral head, necrotic areas, and cystic lesions were then exported to the 3-matic software (version 13.0; Materialise, Leuven, Belgium). Using a software tool in the 3-matic software, the femoral head and cystic lesions were divided into eight regions (I-VIII) with the three planes (Figure 4). Because a cystic lesion might be distributed across multiple regions at the same time, we defined the region containing the largest volume of the cystic lesion as its distribution area. To study the relative positional relationship of cystic lesions to normal areas and necrotic areas, we divided them into three types: L1, the cystic lesions are completely located in the necrotic area; L2, the cystic lesions are distributed in both the normal and necrotic areas; and L3, the cystic lesions are completely in the normal area.

Statistical analysis

For the statistical analysis, we use the mean and standard deviation for continuous variables. A proportion was used for categorical variables. Statistical Package for the Social Sciences (version 21.0.0.0; SPSS Inc., USA) was used for the analyses. The location distribution of cystic lesion analysis and the relative positional relationship of cystic lesions to normal areas and necrotic areas are descriptive in nature.

Results

The characteristics of the enrolled patients are summarised in Table 1. Among all patients, 75 hips were at stage II, 80 hips were at stage III, 26 patients had unilateral ONFH, and 68 patients had bilateral ONFH, of which 7 patients with bilateral ONFH included only one side because the contralateral side was in stage I or stage IV. There were 17 women and 77 men with a mean age of 40 years (range 20–64 years). Of the 155 ONFH hips, 67 hips contained 108 cystic lesions, 38 hips (57%) were complicated by single cysts, and 29 hips (43%) were complicated by multiple cysts. The incidence of cystic lesions in ONFH was 43% (67/155).

Three-dimensional images of each cystic lesion, necrotic area, and

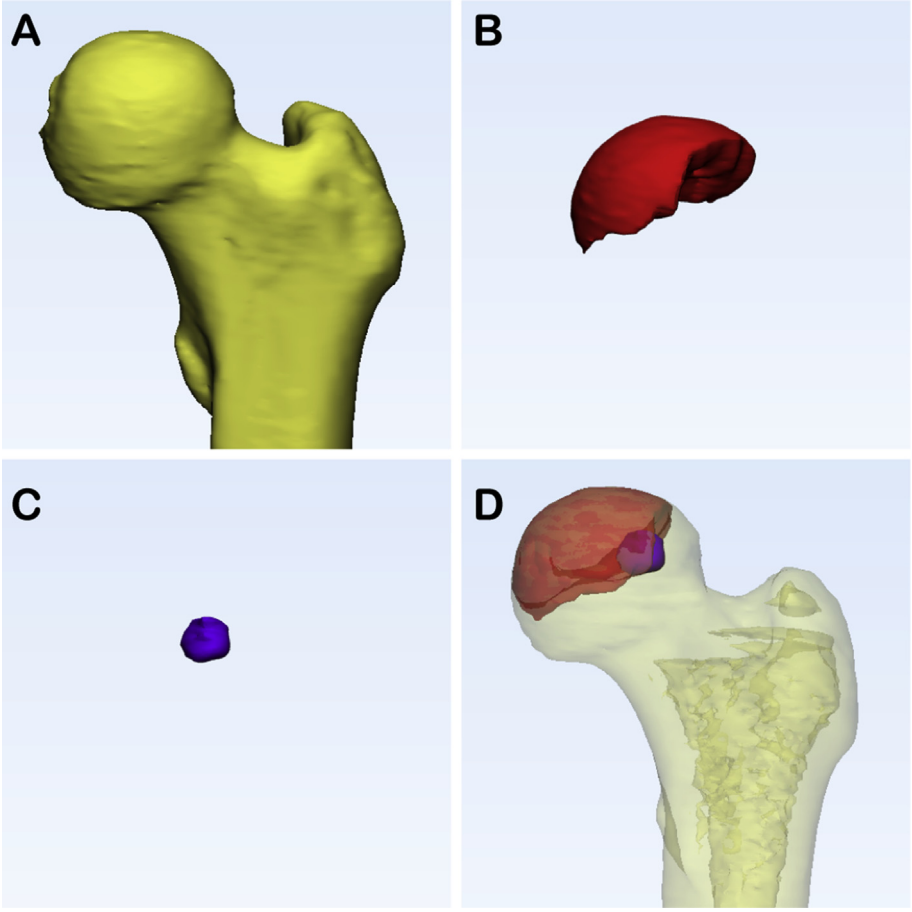

Figure 2. Objects are reconstructed in three dimensions and smoothed using Mimics software (version 21.0; Materialise, Leuven, Belgium) to obtain a three-dimensional structure that is optimally homogeneous and faithful to the patient anatomy. (A), femoral head. (B), necrotic area. (C), cystic lesion, and (D) combination picture.

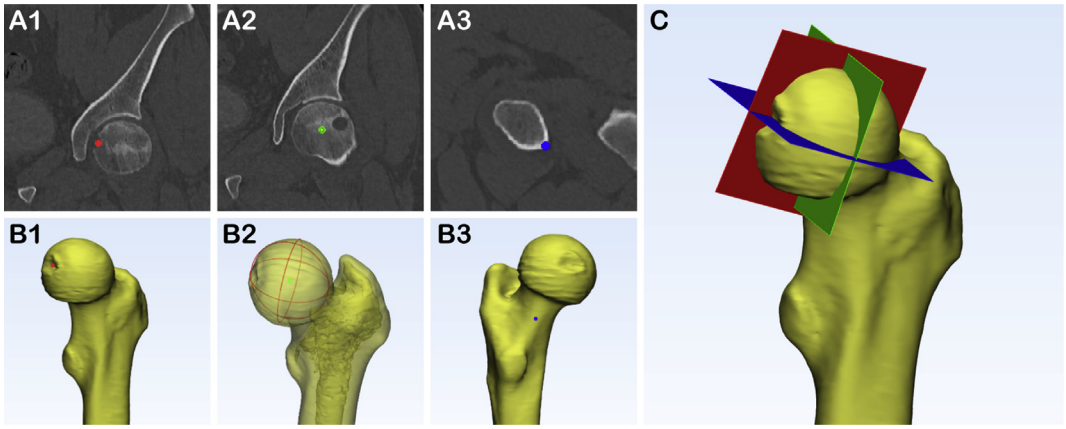

Figure 3. Determination of three mutually perpendicular segmentation planes. (A1-A3, B1-B3) The red point (A1, B1), green point (A2, B2), and blue point (A3, B3) indicate the positions of the centre of femoral head fovea, the centre of the femoral head and the centre of the calcar in the CT plane and the three-dimensional structure respectively. (C) Plane 1 (red plane) was obtained, which included the centre of the femoral head, the centre of femoral head fovea and the centre of the calcar. Plane 2 (blue plane) is perpendicular to Plane 1 and passes through the centre of the femoral head and the centre of femoral head fovea. Plane 3 (green plane) passes through the centre of the femoral head and is perpendicular to Plane 1 and Plane 2. (For interpretation of the references to colour in this figure legend, the reader is referred to the Web version of this article.)

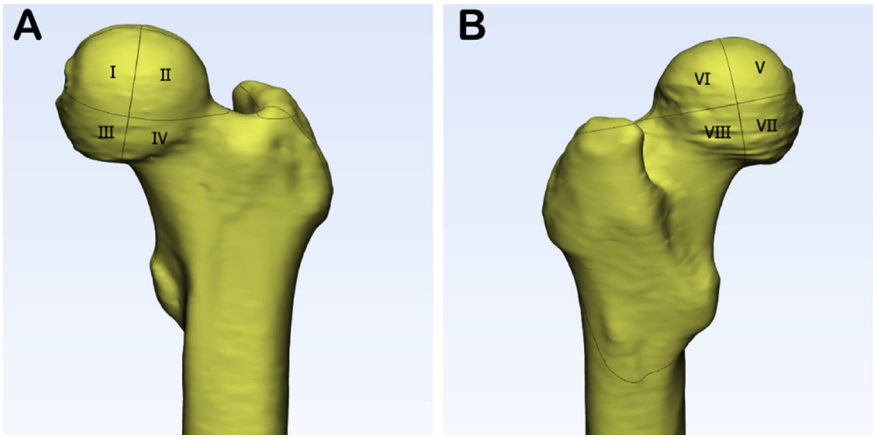

Figure 4. The femoral head and cystic lesions are divided into eight regions (I-VIII) by -three mutually perpendicular planes. (A) I-IV represents superomedial region, superolateral region, inferomedial region, and inferolateral region in the anterior side of the femoral head respectively. (B) V-VIII represents superomedial region, superolateral region, inferomedial region, and inferolateral region in the posterior side of the femoral head respectively.

Table 1
The baseline characteristics and demographics of the study population.

Variable	Outcome
Age (year, mean ± SD)	40 ± 10
Gender (M/F)	77/17
ARCO staging	
II (%)	75 (48)
III (%)	80 (52)
Hips with ONFH in 2 and 3 stage	155
Unilateral ONFH (%)	26 (28)
Bilateral ONFH (%)	68 (72)
ONFH with cyst (%)	67 (43)
ONFH without cyst (%)	88 (57)
Number of cysts in per femoral head	
Single cyst (%)	38 (57)
Multiple cysts (%)	29 (43)
two cysts	19 (28)
three cysts	8 (12)
four cysts	2 (3)

ARCO = Association Research Circulation Osseous, ONFH = osteonecrosis of the femoral head.

femoral head were reconstructed, and there were five necrotic femoral heads for which we could not accurately obtain necrotic shapes on all levels and thus could not construct three-dimensional models of necrotic area (Supplementary 1). The distribution of cystic lesions in the eight femoral head regions is shown in Table 2. The location of cystic lesions on the hip revealed that there were 14 cystic lesions in region I (13%), 35 in II (32%), 9 in III (8%), 25 in IV (23%), 6 in V (6%), 15 in VI (14%), 4 in VII

Table 2
The distribution of cystic lesions in regions I-VIII in ONFH.

Location	Outcome	
	Number	Percentage (%)
I	14	13
II	35	32
III	9	8
IV	25	23
V	6	6
VI	15	14
VII	4	4
VIII	0	0
Total	108	100

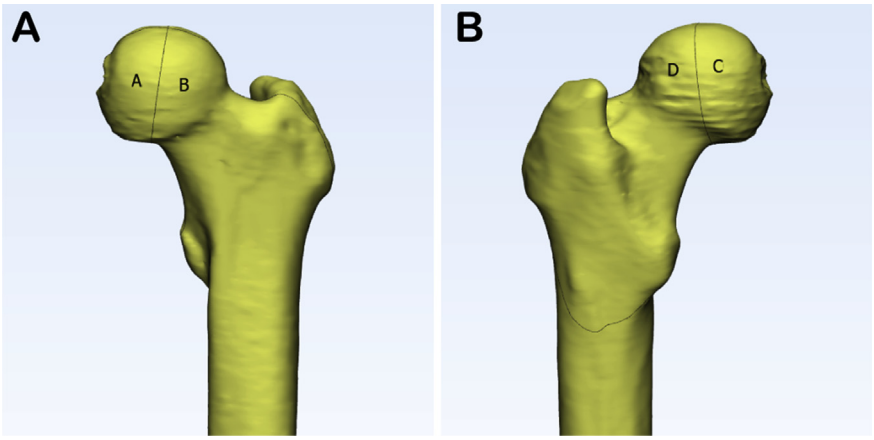

Figure 5. To make the distribution characteristics more obvious, the eight areas are redivided into four areas: anteromedial zone, A (I + III), anterolateral zone, B (II + IV), posterolateral, C (V + VII), and posteromedial, D (VI + VIII). (A) The locations of zone A and B. (B) The locations of zone C and D.

(4%), and 0 lesions in region VIII (0%), indicating that zone II is the region with the largest cyst distribution. We can see that the adjacent zones II and IV contained a significantly higher number of lesions than the other zones did. To make the trend more obvious, we further divided the femoral head into four zones: the anteromedial zone, A (I + III); anterolateral zone, B (II + IV); posteromedial zone, C (V +VII); and posterolateral zone, D (VI + VIII) (Figure 5). The new partitioning method displays a more distinct distribution as follows: there were 24 cystic lesions in zone A (22%), 58 in B (54%), 10 in C (9%), and 16 in D (15%), which indicates that anterolateral zone B was the main distribution area of cystic lesions in hips with ONFH Table 3.

For research on the positional relationship of cystic lesions to necrotic areas and normal areas in a three-dimensional space because there were five necrotic femoral heads containing 8 cystic lesions for which we could not obtain three-dimensional models of the necrotic area, we only obtained 62 cases with 100 cystic lesion data that had acceptable reconstruction quality. We found that there were 18 (18%) cystic lesions in the necrotic area, 4 (4%) in the normal area, and 78 (78%) in between the necrotic and normal areas Table 4.

Discussion

To the best of our knowledge, this is the first study to investigate the distribution of cystic lesions in ONFH on the three-dimensional level. Based on our data, we found that most of the cystic lesions (78%) are located between the normal and necrotic areas. Moreover, most of the cystic lesions that are classified into L1 and L3 are also located near the junction of normal and necrotic areas. In addition, by using our classification system, the cystic lesions were mainly located in regions II (32%) and IV (23%) of the femoral head, and zone B comprising these two regions accounted for 54% of the total number of cystic lesions.

Although it is important to identify and monitor cystic lesions because they accelerate structural collapse, a limited number studies have examined the location characteristics of these lesions [6]. Resnick et al. [10]analysed preoperative radiographs and sectional radiography of surgical specimens removed during total hip replacements and proposed

Table 3
The distribution of cystic lesions in zones A-D in ONFH.

Location	Outcome	
	Number	Percentage (%)
A (I + III)	24	22
B (II + IV)	58	54
C (V +VII)	10	9
D (VI + VIII)	16	15
Total	108	100

Table 4
Distribution characteristics of cystic lesions in necrotic and normal areas.

Type of cyst	Number	Percentage (%)
L1	18	18
L2	78	78
L3	4	4
Total	100	100

that the cystic lesions were located in the superior middle and outer thirds of the femoral head, considered to be its main weight-bearing portion of the femoral head, which is similar to our three-dimensional results (zone B, anterolateral region of the femoral head). However, in contrast to our results that cystic lesions are more likely to be located between the normal and necrotic areas, Resnick's study showed that cystic lesions are located in the necrotic area. This may be because their results were based on superimposed X-ray images of the femoral head, which cannot fully reflect the real three-dimensional relationship.

Compared with Resnick's study, Gao's study based on midcoronal- and midaxial-sectioned CT images improved the accuracy of the study [6]. Their study showed that cystic lesions mainly involve the lateral and central pillars and anterior hip area, which draws similar conclusions as our study. Based on our data, 78% of cystic lesions were Type L2 (presenting at the junction of the necrotic area and the normal area, close to the sclerotic rim), which seems to be a larger proportion than 43% of G2 type (cystic lesions inside the necrotic region and with a connection to the sclerotic rim, as defined in Gao's classification). In addition, our study finds that the proportions of lesions distributed on the anterior side (I-IV) and lateral side (II, IV, VI, VIII), respectively, are 76% and 69%, both of which seem to be slightly higher than the corresponding results in Gao's study (70% and 46%). One possible reason for the difference is that the shapes of the femoral head, necrotic areas, and cystic lesions are irregular, and thus we cannot obtain comprehensive information using only specific layers of CT images. Another reason is some cystic lesions may not be observed on any of the layers (the midcoronal, midaxial, or maximal necrotic lesions) that were selected in Gao's study.

The reason for the specific distribution of cystic lesions remains unclear. Resnick et al. [10]reported that cystic lesions are related to osteoclastic resorption of necrotic trabeculae with fibrous replacement of bone. Gao et al. [6] further suggested that the bone resorption of osteoclasts is due to excessive stress. As shown in Tables 3 and 4, cystic lesions were mostly distributed in zone B (anterolateral region of the femoral head) and were mainly characterised as Type L2 (presenting at the junction of the necrotic area and the normal area, close to the sclerotic rim). Previous studies have shown that the anterolateral region of the femoral head is the main weight-bearing area of the femoral head

[14–16]. In addition, the sclerotic rim is also a stress-concentrated area of the femoral head [12,17,18]. Thus, the cystic lesions in ONFH are mainly located in the stress concentration area of the femoral head. Therefore, based on above findings, we hypothesise that the formation of cystic lesions may relate to stress, similar to the developed of cysts by stress-induced bone resorption in OA [19,20]. The theory suggests that stress-induced microfracture may be the first step in the development of subchondral bone cysts. Secondary effects, such as osteoclast resorption, then induce the cystic lesion itself [20]. Near the sclerotic rim located in the anterolateral area of the femoral head, the peak levels of von Mises stress, which are within the reported range for the maximum compressive strength of trabecular bone, may result in microfracture, as in OA [21,22]. Repeated or increased loading may cause the process to occur again and again, and fragments of disrupted bone are removed by osteoclasts and replaced with fibrous tissue [19,20]. Finite element modelling (FEM) demonstrated that the presence of an intraosseous defect leads to a significant increase in the maximum pericystic stress values under mild static loading, which would promote further bone resorption and subsequent cyst expansion [22]. Furthermore, in OA cysts, pathological changes associated with increased stress could evoke a macrophage response [23]. The macrophages found within the lining of human cysts can contribute to the osteoclastic resorption of subchondral bone surrounding OA cysts by macrophage–osteoclast differentiation, which play a role in the osteolysis associated with enlargement of cysts [23]. Because of the similar tissue elements between cysts in OA and ONFH [9,10], this biological factor might also contribute to promoting the maintenance and expansion of cystic lesions in ONFH. However, we have not further verified this hypothesis and thus need to test it through additional experiments in the future.

ONFH may lead to progressive destruction of the hip joint, although the pathogenesis has not been definitely characterised [24]. The prognosis of ONFH depends mainly on whether the articular surface collapses [4,5]. The location of the necrotic lesion is considered the important factor in collapse [25]. Ohzono et al. [26] indicated that the lesions involving the lateral portion of the weight-bearing surface had the worst prognosis. Nishii et al. [27] reported that lesions located in the anterosuperior portion of the femoral head were a risk factor for collapse. Furthermore, Kubo et al. [28] suggested that ONFH patients with anterior localisation of necrotic lesions can suffer collapse even if the necrotic lesions are medially located. Their results highlighted the importance of anteriorly and laterally located necrotic lesions, respectively. Our study found that cystic lesions are mainly located on the anterolateral side of the femoral head, which might further reduce mechanical strength and accelerate collapse. Moreover, Yu et al. [12]showed that he formation of a sclerotic rim can delay or prevent collapse in osteonecrosis by providing mechanical support for the femoral head. Cystic lesions, most of which are connected to the sclerotic rim, might destroy the integrity of the sclerosis rim and thus reduce protection for necrotic tissue. Therefore, the cystic lesions could further accelerate the collapse of the femoral head. Although the optimal treatment strategy remains controversial, it is generally believed that active joint-preserving treatments before collapse can improve patient prognosis [24]. Considering that cystic lesions can increase the risk of collapse [6], so patients with such lesions should be evaluated carefully and followed up frequently so that the need for surgical intervention can be detected as soon as it arises.

There were some limitations of this study. Firstly, although we showed a more obvious trend of cystic distribution, we only considered the location with the largest cystic variation as the distribution area, which may not accurately indicate the full cystic lesion distribution. Moreover, this study was a single centre study, and the sample size of this study may not be large enough; thus, future studies are still needed to further confirm our conclusions.

Conclusion

Cystic lesions most often occur at the junction of the necrotic area and normal area and are most commonly located in the anterolateral femoral head, which is similar to the distribution of the stress concentration region.

Declarations

Three-dimensional reconstruction images of the cystic lesions, necrotic areas, and femoral head are available in supplementary materials.

Funding

This study was supported by the Natural Science Foundation of China (Funding Number: 81572148).

Compliance with ethical standards

This article was approved by the Medical Ethics Committee of Chinese PLA General Hospital (S2019-019-01).

Conflict of interest

The authors have no conflicts of interest to disclose in relation to this article.

Appendix A. Supplementary data

Supplementary data to this article can be found online at https://doi.org/10.1016/j.jot.2019.10.010.

References

[1] Sugioka Y, Hotokebuchi T, Tsutsui H. Transtrochanteric anterior rotational osteotomy for idiopathic and steroid-induced necrosis of the femoral head. Indications and long-term results. Clin Orthop Relat Res 1992;(277):111–20 [eng].
[2] Patterson RJ, Bickel WH, Dahlin DC. Idiopathic avascular necrosis of the head of the femur. A study of fifty-two cases. J Bone Jt Surg Am 1964;46:267–82 [eng].
[3] Baig SA, Baig MN. Osteonecrosis of the femoral head: etiology, investigations, and management. Cureus 2018;10(8):e3171 [eng].
[4] Ohzono K, Saito M, Takaoka K, Ono K, Saito S, Nishina T, et al. Natural history of nontraumatic avascular necrosis of the femoral head. J Bone Jt Surg Br 1991;73(1):68–72 [eng].
[5] Lieberman JR, Berry DJ, Mont MA, Aaron RK, Callaghan JJ, Rajadhyaksha AD, et al. Osteonecrosis of the hip: management in the 21st century. Instr Course Lect 2003;52:337–55 [eng].
[6] Gao F, Han J, He Z, Li Z. Radiological analysis of cystic lesion in osteonecrosis of the femoral head. Int Orthop 2018;42(7):1615–21 [eng].
[7] Hamada H, Takao M, Sakai T, Sugano N. Subchondral fracture begins from the bone resorption area in osteonecrosis of the femoral head: a micro-computerised tomography study. Int Orthop 2018;42(7):1479–84 [eng].
[8] Sugano N, Atsumi T, Ohzono K, Kubo T, Hotokebuchi T, Takaoka K. The 2001 revised criteria for diagnosis, classification, and staging of idiopathic osteonecrosis of the femoral head. J Orthop Sci : Off J Japan Orthopaed Assoc 2002;7(5):601–5 [eng].
[9] McCollum DE, Mathews RS, O'Neil MT. Aseptic necrosis of the femoral head: associated diseases and evaluation of treatment. South Med J 1970;63(3):241–53 [eng].
[10] Resnick D, Niwayama G, Coutts RD. Subchondral cysts (geodes) in arthritic disorders: pathologic and radiographic appearance of the hip joint. AJR Am J Roentgenol 1977;128(5):799–806 [eng].
[11] Escudier JC, Ollivier M, Donnez M, Parratte S, Lafforgue P, Argenson JN. Superimposition of maximal stress and necrosis areas at the top of the femoral head in hip aseptic osteonecrosis. Orthop Traumatol Surg Res: OTSR 2018;104(3):353–8 [eng].
[12] Yu T, Xie L, Chu F. A sclerotic rim provides mechanical support for the femoral head in osteonecrosis. Orthopedics 2015;38(5):e374–9 [eng].
[13] Poole KE, Mayhew PM, Rose CM, Brown JK, Bearcroft PJ, Loveridge N, et al. Changing structure of the femoral neck across the adult female lifespan. J Bone Miner Res:Off J Am Soc Bone Min Res 2010;25(3):482–91 [eng].
[14] Yoshida H, Faust A, Wilckens J, Kitagawa M, Fetto J, Chao EY. Three-dimensional dynamic hip contact area and pressure distribution during activities of daily living. J Biomech 2006;39(11):1996–2004 [eng].
[15] Bergmann G, Graichen F, Rohlmann A. Hip joint loading during walking and running, measured in two patients. J Biomech 1993;26(8):969–90 [eng].
[16] Michaeli DA, Murphy SB, Hipp JA. Comparison of predicted and measured contact pressures in normal and dysplastic hips. Med Eng Phys 1997;19(2):180–6 [eng].

[17] Chen Z, Xu Y, Qi Z, Zho J. The formation and function of the sclerosis rim in the femoral head: a biomechanical point of view. Med Eng Phys 2015;37(12):1125–32 [eng].
[18] Karasuyama K, Yamamoto T, Motomura G, Sonoda K, Kubo Y, Iwamoto Y. The role of sclerotic changes in the starting mechanisms of collapse: a histomorphometric and FEM study on the femoral head of osteonecrosis. Bone 2015;81:644–8 [eng].
[19] Ondrouch AS. Cyst formation IN osteoarthritis. J Bone Jt Surg Br 1963;45(4):755–60 [eng].
[20] Durr HD, Martin H, Pellengahr C, Schlemmer M, Maier M, Jansson V. The cause of subchondral bone cysts in osteoarthrosis: a finite element analysis. Acta Orthop Scand 2004;75(5):554–8 [eng].
[21] Rohl L, Larsen E, Linde F, Odgaard A, Jorgensen J. Tensile and compressive properties of cancellous bone. J Biomech 1991;24(12):1143–9 [eng].
[22] McErlain DD, Milner JS, Ivanov TG, Jencikova-Celerin L, Pollmann SI, Holdsworth DW. Subchondral cysts create increased intra-osseous stress in early knee OA: a finite element analysis using simulated lesions. Bone 2011;48(3):639–46 [eng].
[23] Sabokbar A, Crawford R, Murray DW, Athanasou NA. Macrophage-osteoclast differentiation and bone resorption in osteoarthrotic subchondral acetabular cysts. Acta Orthop Scand 2000;71(3):255–61 [eng].
[24] Zalavras CG, Lieberman JR. Osteonecrosis of the femoral head: evaluation and treatment. J Am Acad Orthop Surg 2014;22(7):455–64 [eng].
[25] Chen L, Hong G, Fang B, Zhou G, Han X, Guan T, et al. Predicting the collapse of the femoral head due to osteonecrosis: from basic methods to application prospects. J Orthopaed Transl 2017;11:62–72 [English].
[26] Ohzono K, Saito M, Sugano N, Takaoka K, Ono K. The fate of nontraumatic avascular necrosis of the femoral head. A radiologic classification to formulate prognosis. Clin Orthop Relat Res 1992;(277):73–8 [eng].
[27] Nishii T, Sugano N, Ohzono K, Sakai T, Sato Y, Yoshikawa H. Significance of lesion size and location in the prediction of collapse of osteonecrosis of the femoral head: a new three-dimensional quantification using magnetic resonance imaging. J Orthop Res : Off Pub Orthopaed Res Soc 2002;20(1):130–6 [eng].
[28] Kubo Y, Motomura G, Ikemura S, Sonoda K, Hatanaka H, Utsunomiya T, et al. The effect of the anterior boundary of necrotic lesion on the occurrence of collapse in osteonecrosis of the femoral head. Int Orthop 2018;42(7):1449–55 [eng].